On the heat waves over India and their future projections under different SSP scenarios from CMIP6 models

Article

Published Version

www.reading.ac.uk/centaur

CentAUR

Central Archive at the University of Reading

Reading's research outputs online

RESEARCH ARTICLE

On the heat waves over India and their future projections under different SSP scenarios from CMIP6 models

Marc Norgate[1,2] | P. R. Tiwari[1,2] | Sushant Das[3,4] | D. Kumar[5]

[1]Centre for Atmospheric and Climate Physics Research, University of Hertfordshire, Hatfield, UK

[2]Centre for Climate Change Research, University of Hertfordshire, Hatfield, UK

[3]Department of Meteorology, Stockholm University, Stockholm, Sweden

[4]Department of Earth and Atmospheric Sciences, National Institute of Technology Rourkela, Rourkela, Odisha, India

[5]National Centre for Atmospheric Science, Department of Meteorology, University of Reading, Reading, UK

Correspondence
P. R. Tiwari, Centre for Atmospheric and Climate Physics Research, University of Hertfordshire, Hatfield, UK.
Email: p.r.tiwari@herts.ac.uk

Funding information
Research England: QR Strategic Priorities Funding (QR-SPF), Grant/Award Number: 274762653

Abstract

Thirteen Coupled Model Intercomparison Project phase 6 (CMIP6) models were employed to simulate mean, maximum, and minimum temperature across 7 homogenous temperature regions of India for both annual and summer season (June, July, and August (JJA)). The model fidelity was assessed by comparing them with observed Climate Research Unit temperature dataset. The JJA multi-model ensemble for the present (1981–2014) suggests large warm biases in the temperature. Although the models could simulate the spatial variability of the mean and maximum temperature over most of the homogeneous regions, they do not compare well for representing the temporal variability. We also found, that although different individual models have strengths and weaknesses in representing spatial and temporal temperature characteristics over India, a few of the models perform better than the others. For example, CNRM-CM6 could better represent the spatial temperature patterns however they struggle in capturing the temporal variability. HadGEM3-GC31-LL, KACE-1-0G, and UKESM1-0-LL are comparably the best-performing models for temporal temperature features over India. The annual maximum temperature during far future period is projected to increase by 1.5°C, 2.3°C, and 4.1°C for Socioeconomic Pathways (SSPs) SSP1-2.6, SSP2-4.5, and SSP5-8.5 respectively. At regional scales, JJA mean temperature for SSP5-8.5 revealed significant increases in Interior Peninsula (3.8°C), Western Himalaya (5.6°C), Northwest (3.9°C), West Coast (3.6°C), East Coast (3.6°C), Northeast (3.6°C), and North Central (3.8°C), highlighting the Western Himalaya's heightened sensitivity. Further, heat wave frequency is projected to rise, with the northern territories (NW, NC, NE, and part of IP) most affected, anticipating week-long heat waves affecting around 50% of India's population

under stronger SSPs. Such unprecedented impacts seem to be less profound in case of abatement scenarios such as the SSP1-2.6. Our findings support the urgent need for more ambitious mitigation and adaptation strategies to alleviate the public health impacts of climate change.

KEYWORDS

climate change, CMIP6, extremes, heat waves, India, SSP

1 | INTRODUCTION

There is high confidence that climate change has caused irreversible damage to terrestrial, freshwater, coastal, and open marine ecosystems. A warming of approximately 0.85°C has occurred globally in the last 40 years and without sufficient mitigation strategies global surface temperatures will continue to rise. It is extremely likely that human influence is responsible for the rise in global temperature as well as an increase in extreme events such as warm temperature extremes (IPCC, 2022).

South Asia is one of the most vulnerable regions in the world to the impacts of climate change (Sivakumar & Stefanski, 2010) with signs of warming trends and a consistent increase in temperature extremes (IPCC, 2022). The climate change have been shown to affect the food production, putting this region at risk of a food shortage by 2030 and creating food security concerns in the future (Acharya et al., 2014; Bandara & Cai, 2014). Extreme temperatures, heavy rainfall, flooding, and droughts negatively affect agriculture and can sometimes even destroy harvests (Gornall et al., 2010). India's population is particularly vulnerable to extreme temperatures and an increase in heat wave severity has been linked to an increase in heat-related mortality over India (Mazdiyasni et al., 2017).

Heat waves have caused many deaths over India in the last 100 years (De et al., 2005). Mortality related to heat waves in India has increased between 1970 and 2019. The impact of heat waves compared to other extreme weather events varies per state. For instance, Andhra Pradesh is the most affected where the mortality rate due to heat waves increased by 60% followed by Odisha with an increase of 20% (Ray et al., 2021). Most of the heat waves in India usually occur in the pre-monsoon season (April, May, and June) and can cover a large portion of the country (Pai et al., 2013). However, the high temperatures can still persist during the summer monsoon (June, July, and August, JJA) season and therefore it is critical to estimate such occurrences as there is possible climate shift in future scenarios. For example, the monsoon precipitation that occurs actively during JJA over India exhibits a temporal shift in onset dates as well

as the precipitation maxima under RCP 8.5 (Ashfaq et al., 2021; Shahi et al., 2021). The dryness induced in the future could inculcate extreme temperature conditions over India during summer monsoon season.

There is a link between the warming of the Indian Ocean and El-Nino events with heat waves over India (Rohini et al., 2016). The surface temperature of the Indian Ocean is projected to continue to rise in the future (Pattnayak et al., 2017) increasing the likelihood of heat waves over India in the near future. India has a population of over 1.3 billion putting a large portion of the world's population at risk to an increase in extreme temperature events. The most densely populated parts of India are in the Indo-Gangetic plain where approximately half the population lives.

A rise in temperature can be seen globally and it is likely that heat waves have increased in large parts of Asia (IPCC, 2022). Heat waves are a type of extreme weather event, generally defined as an extended period of extreme temperature (Perkins & Alexander, 2013). The frequency, intensity, and duration of extreme heat events have increased globally (Perkins & Alexander, 2013) and South Asia (Dong et al., 2021), which is likely caused by an increase in anthropogenic emissions (Collins et al., 2013; Meehl & Tebaldi, 2004; Pattnayak et al., 2017). Zhao et al. (2019) suggest that these extreme heat events will continue to increase into the future under the RCP 8.5 scenario. They have a significant impact on human health (Arbuthnott & Hajat, 2017; Haines et al., 2006; Patz et al., 2005; Zeng et al., 2016) and have caused many deaths globally, with a greater impact on the elderly, women, and those suffering from chronic respiratory disorders (Dippoliti et al., 2010). This poses a risk to the world's population, especially those in developing countries who will struggle to mitigate this increase in heat wave severity.

Considering such risks to the large population over a vulnerable region like south Asia, it becomes important to investigate the utility of the available modelling tools for understanding the present and future climate change. To aid this, a wide range of climate model simulations are produced through the coordinated efforts worldwide. Coupled Model Intercomparison Project (CMIP) has been

around since the mid 1990s and makes use of general circulation models (GCMs) simulations to improve our understanding of the climate system (Stouffer et al., 2017). CMIP models have received many improvements over the years such as improved resolution, improvements in the representation of the physical processes, and different climate forcings. Representative Concentration Pathways (RCPs, Moss et al., 2010) were introduced in CMIP5 (Taylor et al., 2012) to explore different future scenarios for different radiative forcing pathways. In the present work we will be using the latest Coupled Model Intercomparison Project 6 (CMIP6; Eyring et al., 2016) dataset over India which has been used in many studies globally looking at both temperature and precipitation (Almazroui et al., 2021; Maharana et al., 2018; Pattnayak et al., 2019; You et al., 2016). One of the most notable additions compared to CMIP5 are the Shared Socioeconomic Pathways (SSPs, Riahi et al., 2017) which represent five different narratives for future socioeconomic scenarios (O'Neill et al., 2017). The main aim of this paper is to study present and future changes (near and far future) in mean, max, and min temperature over India's homogeneous temperature regions using state-of-the-art CMIP6 models.

2 | DATA AND METHODOLOGY

13 CMIP6 models (see Table 1) are used in investigating the maximum, mean, and minimum temperature over India and its seven homogeneous temperature regions (Figure 1). The Indian Institute of Tropical Meteorology at Pune has defined these seven homogenous regions which are specified based on spatial and temporal variations of surface air temperature (Dash & Mamgain, 2011). The seven homogenous temperature regions are the Western Himalaya (WH), Northwest (NW), North Central (NC), North East (NE), West Coast (WC), East Coast (EC), and Interior Peninsula (IP) regions. Similar homogenous regions have been used when assessing temperature over India (Dileepkumar et al., 2018). The CMIP6 data used in this work can be found from the CMIP6 database (https://esgf-node.llnl.gov/search/cmip6/). The historical analysis is from 1984 to 2014 and this time period is used to examine the performance of the models in representing different characteristics of temperature variations over the region. Besides the individual experiment, we also compute the multi-model ensemble (MME) from the 13 CMIP6 models. Daily data is required for the temperature variables for the computation of ETCCDI heat extremes (https://etccdi.pacificclimate.org/list_27_indices.shtml) and can be seen in Table 2. Out of 13 models, 9 models had daily data archived therefore, we used them for the calculating the heat extremes and MME. The models used in the daily data MME are CMCC, CNRM, GFDL, HadGEM, INM, KACE, MIROC6, MPI, and UKESM. The method for projecting these extreme temperatures is shown in Figure 2.

All models have been re-gridded to the observed grid (Climatic Research Unit (CRU) data, Harris et al., 2013) which has resolution of $0.5° \times 0.5°$. The monthly maximum, mean, and minimum near-surface air temperature from CRU is used to evaluate the individual model and their MME. CRU is a well-trusted source of historical observations (Mitchell & Jones, 2005) and has been used

TABLE 1 CMIP6 ESMs used in the present work.

| Model	Country	Horizontal resolution (lon and lat)	Model vertical levels (km)
ACCESS-CM2	Australia	192 × 144	85
CANESM5-CanOE	Canada	128 × 64	49
CMCC-ESM2	Italy	288 × 192	30
CNRM-CM6-1	France	362 × 294	75
FIO-ESM-2-0	China	192 × 288	26
GFDL-ESM4	USA	360 × 180	49
GISS-E2-1-H	USA	144 × 90	40
HadGEM3-GC31-LL	UK	192 × 144	85
INM-CM5-0	Russia	180 × 120	73
KACE-1-0-G	South Korea	192 × 144	85
MIROC6	Japan	256 × 128	81
MPI-ESM1-2-LR	Germany	192 × 96	47
UKESM1-0-LL	UK	192 × 144	85
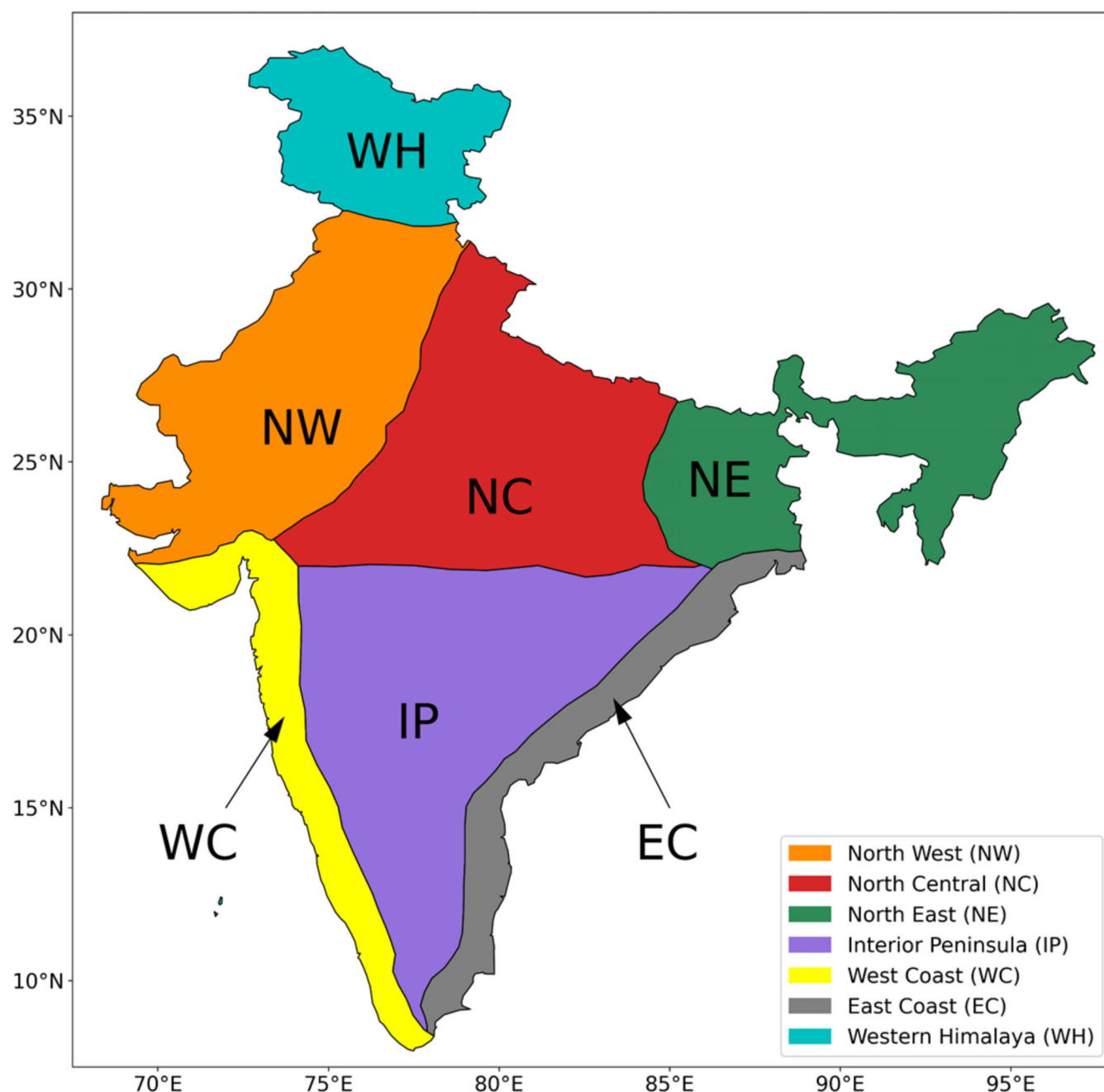
FIGURE 1 Study area and different temperature homogenous regions over India. [Colour figure can be viewed at wileyonlinelibrary.com]

in many previous studies (Dileepkumar et al., 2018; Kanda et al., 2020; Kumar et al., 2013; Maharana et al., 2018; Panda et al., 2020; Pattnayak et al., 2017; Ullah et al., 2022).

We first evaluate the models in terms of their capabilities in representing the climatological mean annually and during the summer season (JJA), mean annual cycle, Taylor's metrics, and representation of the probability distribution over individual temperature homogeneous regions over India. To further understand the model's

capabilities in representing the mean patterns spatially, we compute the differences of the mean for the present climate (with respect to observation) and future climate (with respect to present climate). To assess the changes during the future, we make use of three different SSP namely: SSP1-2.6, SSP2-4.5, and SSP5-8.5 where SSP1-2.6 represents a 'green road', SSP5-8.5 represents fossil-fuelled development and SSP2-4.5 represents a middle road (Riahi et al., 2017). The SSPs used represent low (SSP1-2.6), medium (SSP2-4.5), and high (SSP5-8.5)

TABLE 2 Heat wave variables calculated using ETCCDI (https://etccdi.pacificclimate.org/list_27_indices.shtml).

| Consecutive summer days index per summer season	Warm days percent wrt 90th percentile of the summer season	Warm spell days index wrt 90th percentile of the summer season	Heat waves per summer season	Heat wave duration index wrt the mean of the summer season
The largest number of consecutive summer days per summer season. In this case a summer day is where $T_{max} > 31°C$ (31°C is the mean of T_{max} for the historical period)	The per centage of time where $T_{mean} > T_{mean}90$. $T_{mean}90$ is the 90th percentile of daily T_{mean} for a 5-day window centered on each calendar day for the historical period	The number of days where $T_{mean} > T_{mean}90$ in intervals of 6 consecutive days. $T_{mean}90$ is the same as warm days percent	The number of heat waves equal to, or longer than n days per summer season. In this case a heat wave is where $T_{max} > T_{max}Norm + 5°C$ for n consecutive days. $T_{max}Norm$ is the mean of T_{max} of a 5-day window centered on each calendar day for the historical period. We calculated results for $n = 3, 5,$ and 7 days	Number of heat wave days equal to, or longer than n days per summer season. Uses the same heat wave definition as heat waves per summer season.
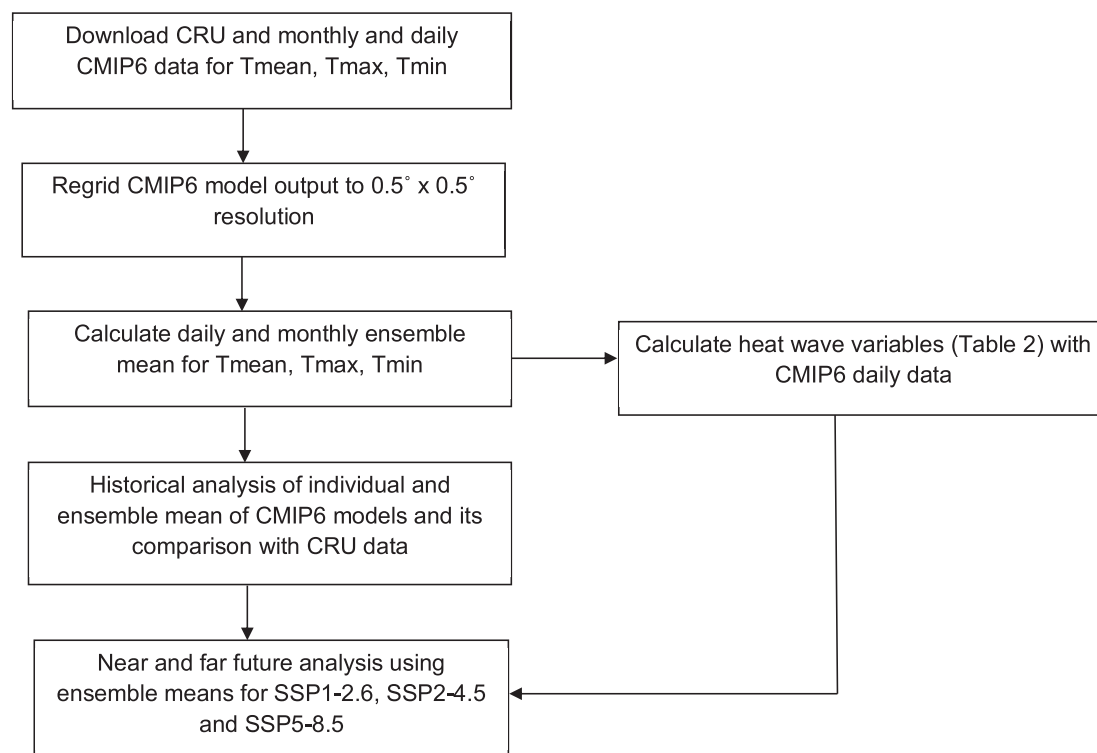
FIGURE 2 Schematic diagram showing the methodology used for the analysis.

emission scenarios making SSP5-8.5 the most aggressive scenario in terms of emissions. To highlight the spatial heterogeneity in the differences, we compute the significance of differences in the mean by applying the student *t*-test and have identified the areas having significant differences at 95% level. All SSPs represent the future time period 2015–2100 and have been split into near-future [NF (2030–2060)] and far-future [FF (2070–2100)] to evaluate future changes in maximum, mean, and minimum temperature over India. We looked at projected changes in annual and seasonal temperatures. To analyse future changes in temperature distribution over India and different homogeneous regions, we used spatial, time series, and probability density function (PDF) figures using the SSP scenarios. Furthermore, we have used CDO

(Schulzweida, 2021) to compute different heat wave variables which is shown in Table 2.

3 | RESULTS

Figures 3 and 4 show the biases in MME and individual CMIP6 models in simulating annual and JJA mean temperatures over the homogenous temperature regions of India. The annual Tmean shows large variation of hot and cold biases for individual models. MIROC6 (Figure 3n) has a very high warm bias most notably over the NW region, whereas CNRM (Figure 3e) and GFDL (Figure 3i) have a cold bias over almost all of India

compared to the observations. For JJA Tmean (Figure 3) there are larger warm biases in most models when compared to annual Tmean (Figure 3). MIROC6 consistently shows the largest warm bias again in the NW region. The CANESM and GISS models have a much higher warm bias to the east of the NC and IP regions compared to their annual counterparts. These models are likely contributing to the biases of the MME and there is large inter-model variability over the different homogenous regions. Using the MME reduces the biases overall, especially when studying long-term climate trends for both annual and JJA time periods.

The observed climatology of annual maximum, mean and minimum (Tmax, Tmean, and Tmin) over the
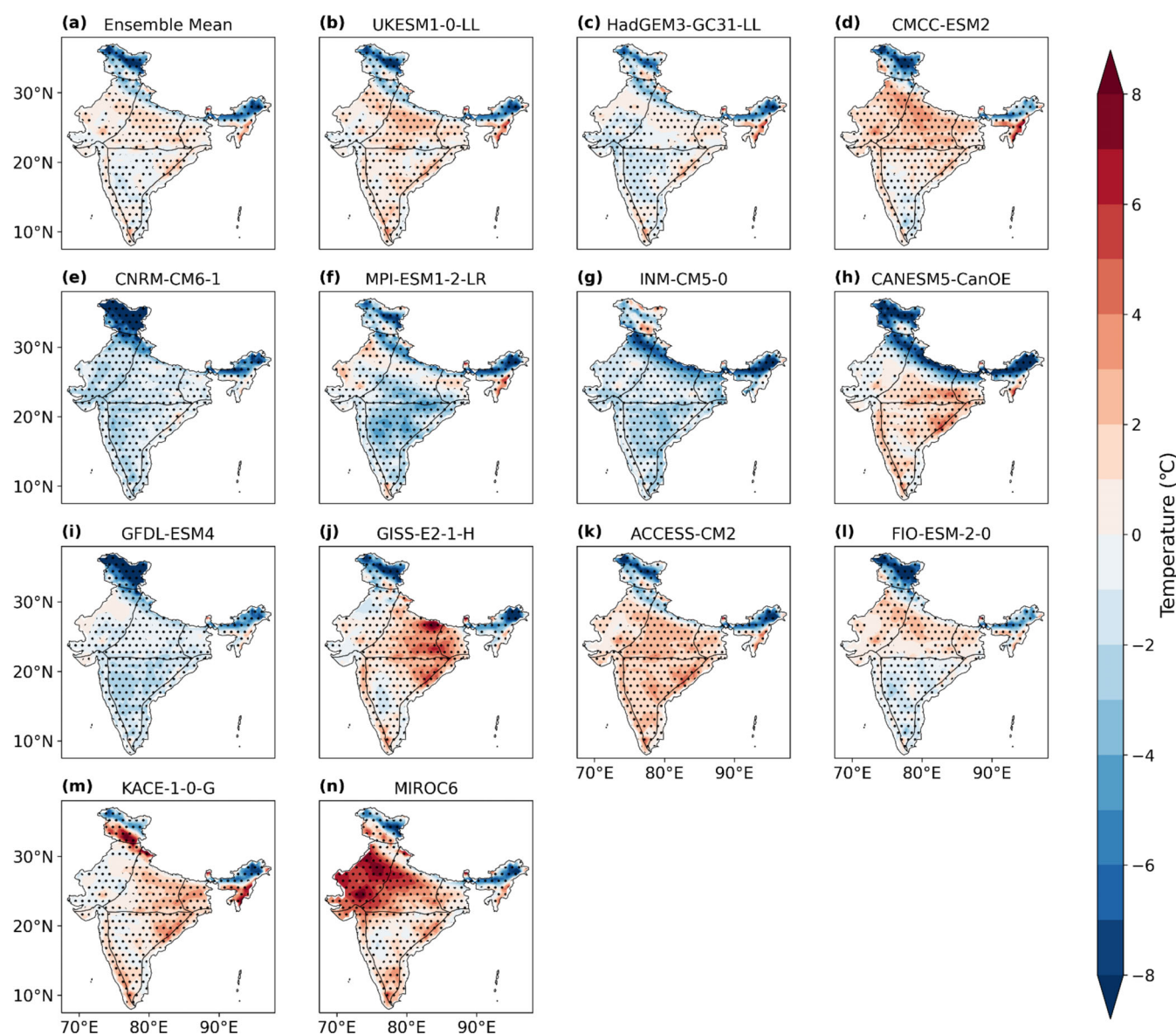

FIGURE 3 Annual mean near surface temperature difference of models compared to observation for the period 1984–2014. Ensemble mean of 13 CMIP6 models (a) and individual CMIP6 models used in ensemble (b)–(n). The dots represent the grid points with significant differences at 95% significance level. [Colour figure can be viewed at wileyonlinelibrary.com]
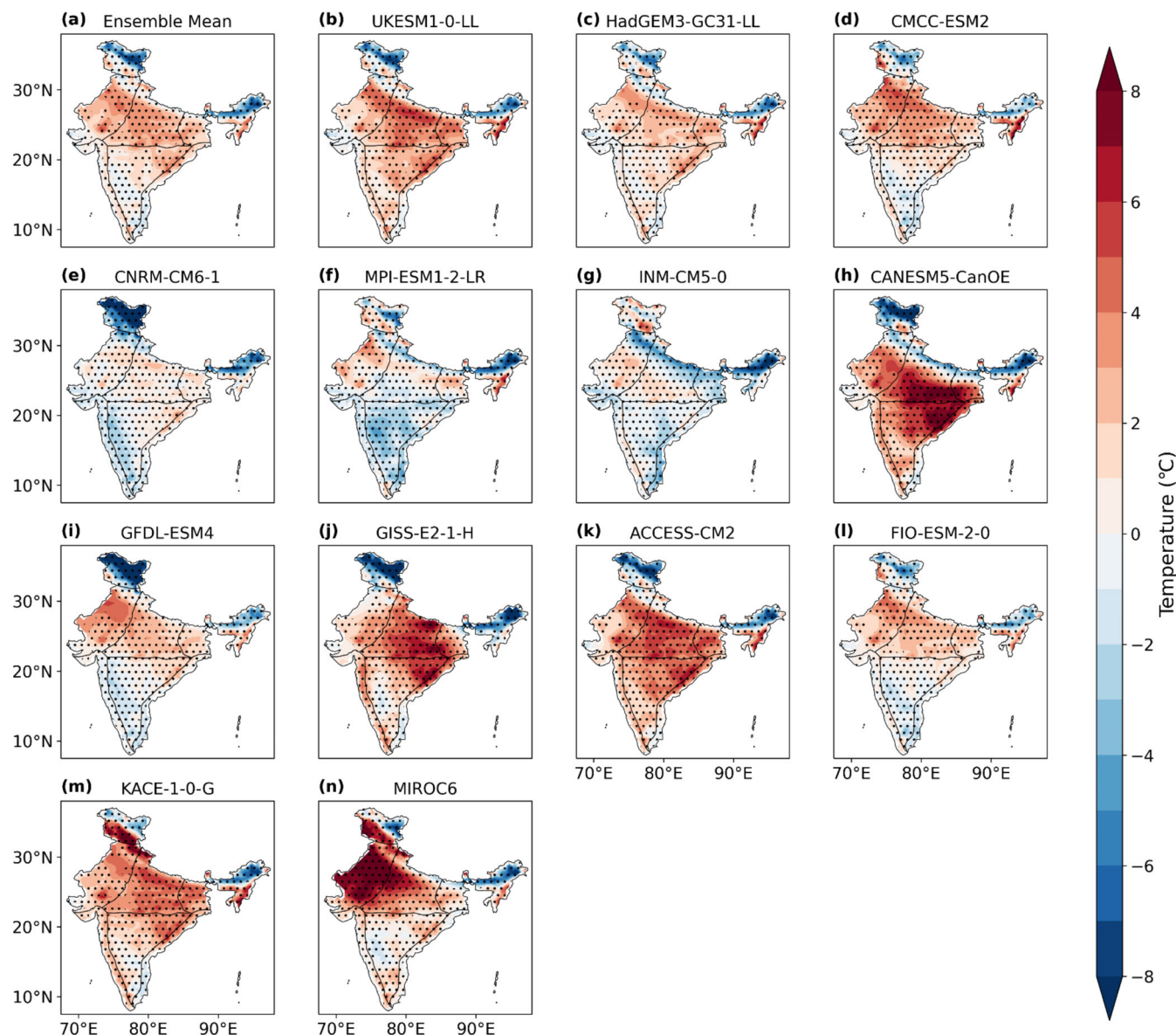
FIGURE 4 JJA mean near surface temperature difference of models compared to observation for the period 1984–2014. Ensemble mean of 13 CMIP6 models (a) and individual CMIP6 models used in ensemble (b)–(n). The dots represent the grid points with significant differences at 95% significance level. [Colour figure can be viewed at wileyonlinelibrary.com]

homogenous temperature regions of India is shown in Figure S1a, d, g and MME (Figure S1b, e, h). The annual temperature ranges from below 5 to 37°C for the entirety of India, with the highest temperatures being from the NW (37°C) and IP (36°C). The difference between the MME and observed data can be seen in Figure S1c, f, i. Generally, the models are good at representing the temperature over India as there are significant values (at 95% significance level) in all regions. The NC region results are mostly significant for annual Tmax and Tmean but show much less significant values when looking at Tmin. There is a large cold bias (>5°C) from the models over the northernmost regions for Tmax (Figure S1a–c),

Tmean (Figure S1d–f), and Tmin (Figure S1g–i). This might be related to the snow cover, the aspect, slope, and complex topography of these regions, and the coarser resolution of these GCMs cannot capture (Das et al., 2021; Tiwari et al., 2016, 2017). A larger warm bias (up to 3°C) from the models can be seen in the Tmax mostly over the NC, NW, and NE regions, whereas the Tmin has mostly a cold bias over these. There is a high aerosol load over the Indo-Gangetic plains which stretches over these three regions (Dey and Di Girolamo, 2010) and could explain the warm biases seen which are not considered in this set of CMIP6 models. A similar analysis for the JJA period (Figure S2) shows much larger warm biases for Tmax,
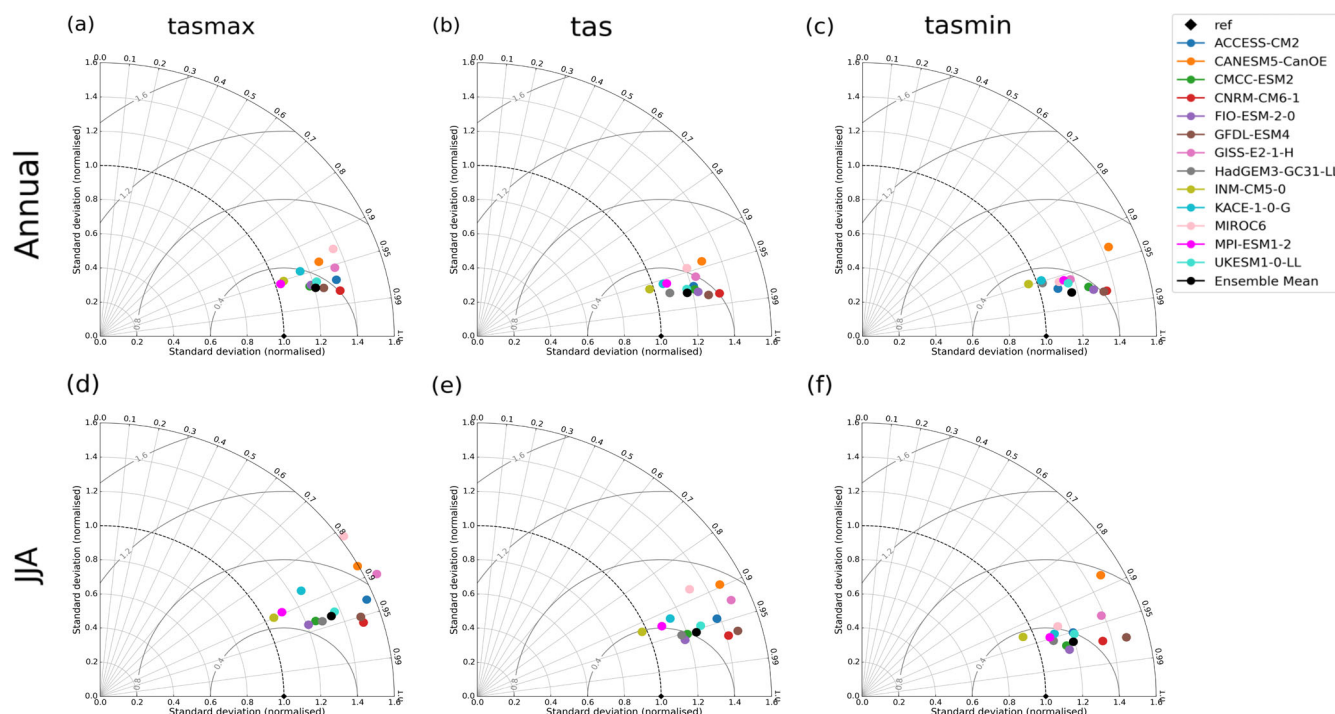
FIGURE 5 Taylor diagram showing the annual (a)–(c) and JJA (d)–(f) maximum (a), (d) mean (b), (e) and minimum (c), (f) temperature over India. The correlation coefficient and normalized standard deviation for 13 CMIP6 models compared to observations are shown. The grey curved lines show the root mean square error (RMSE). [Colour figure can be viewed at wileyonlinelibrary.com]

Tmean, and Tmin. This further suggests that the MME is substantially overestimating both hot and cold temperatures in the present.

A Taylor diagram (Taylor, 2001) is presented in Figure 5. In this diagram, the performance of individual models in simulating Tmax, Tmean, and Tmin during the annual (Figure 5a–c) and JJA (Figure 5d–f) periods in terms of the correlation coefficient (CC), root mean square error (RMSE) and normalized standard deviation (SD) is shown. A model that is closest to an SD of 1 and CC of 1 is closest to the observed values. Models perform reasonably well when capturing Tmax, Tmean, and Tmin for both time periods and the models tend to give results closer to observation for annual compared to JJA. There is more of a spread in CC and SD values for JJA compared to annual which highlights the inter-model differences. Almost all models have a CC of over 0.95 for the annual period and over 0.9 for JJA. The SD is generally between 1 and 1.4 for all models for both annual and JJA. Most models have an RMSE of less than 0.4 for the annual period but have a larger RMSE of between 0.4 and 0.8 for JJA. For JJA Tmin, RMSE is smallest for all models. The MME outperforms the individual model experiments and is closer to the observed values in most cases. The FIO and CMCC models perform comparatively better during the JJA period with the FIO model outperforming the MME. The performance of CANESM5 and

MIROC6 models in simulating temperature over India is poor compared to the rest of the CMIP6 models used in this study.

The models do well at simulating temperature spatially however, they struggle much more temporally for JJA tas and tasmax (Figure 6). When looking at the spatial patterns of temperature (Figure 6a, b), models show good CC (0.7+) for the WH, NW, WC, NC, and NE regions. The IP shows a slightly lower CC of 0.5 compared to other regions. All models appear to struggle with the EC region with the lowest values being from the CanESM, KACE, and GISS models with a correlation of −0.5 for both tas and tasmax. Moving onto temporal correlations, almost all models give low values for all regions. The only models that give CC values over 0.5 are the HadGEM, KACE, and UKESM models. This is the same for both temporal tas and tasmax. These results suggest that the models are much better at representing the temperature spatially as opposed to temporally when looking at the individual temperature homogenous regions.

The PDF distributions of the Tmean over India using present and three different SSP scenarios for both annual and JJA periods are shown in Figure 7. The MME underestimates the annual Tmean with a difference of 0.5°C and overestimates the JJA Tmean with a difference of 2.1°C when compared to observed values. SSP1-2.6,
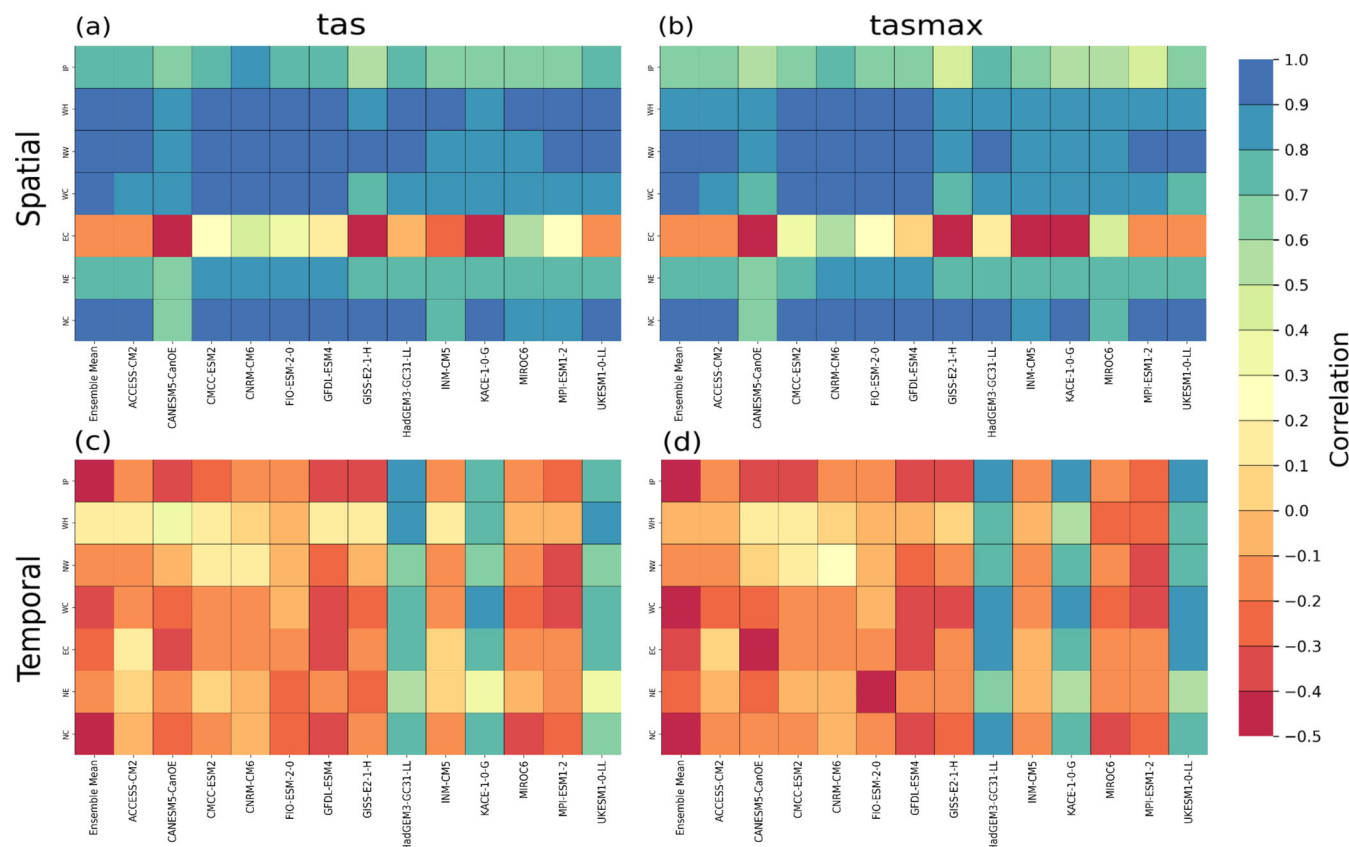
FIGURE 6 Diagonal correlation matrix for JJA Tmean (a), (c) and Tmax (b), (d) over the Indian temperature homogenous regions. Correlation is shown for the individual models (columns 2–14) and the ensemble mean of these models (column 1) compared to observed values for the historical period (1984–2014). Fig a and b show the spatial correlation and fig c and d show the temporal correlation. [Colour figure can be viewed at wileyonlinelibrary.com]

SSP2-4.5, and SSP5-8.5 are split into NF and FF, with a shift in annual Tmean of 0.8, 0.9, and 1.2°C for NF, respectively, and 1.1, 2, and 4°C for FF, respectively, compared to observed values. FF SSP5-8.5 shows the largest shift in Tmean and a noticeably higher temperature distribution compared to all other scenarios. The difference between NF and FF SSP5-8.5 is also very large compared to other scenarios with a difference of 2.8°C compared to 0.3°C for SSP1-2.6 and 1.1°C for SSP2-4.5. This suggests that under SSP5-8.5 there will be much more warming towards the end of the century. Similarly, when comparing JJA Tmean with observed values, a shift of 2.1, 2.2, and 2.4°C can be seen for NF and 2.3, 3.2, and 4.9°C can be seen for FF SSP1-2.6, SSP2-4.5 and SSP5-8.5, respectively. Both annual and JJA show similar increases in Tmean between NF and FF SSP1-2.6, SSP2-4.5, and SSP5-8.5 with FF SSP5-8.5 showing a noticeably warmer climate compared to present day. The JJA shift in Tmean is larger for both NF and FF compared to the annual period. The NF SSP5-8.5 distribution shows a warmer climatology than FF SSP1-2.6 for both annual and JJA periods suggesting that with sufficient mitigation we can

significantly reduce the amount of warming by the end of the century.

Furthermore, the PDF over individual homogeneous regions is discussed in Figure 8 for the JJA and Figure S3 for annual season. For JJA Tmean, the regions with the highest observed Tmean are the NW (30.3°C) and EC (29.5°C). The coldest region is the WH with a Tmean of 11.8°C. For annual Tmean the regions with the highest observed Tmean are the EC (27.6°C) and IP (26.9°C). The coldest region is the WH with a Tmean of 2.4°C. For most regions the historical values from the MME during the annual period are very close to observed values, NW and EC show negligible temperature bias, IP shows a cold bias of 0.2°C, WC shows a warm bias of 0.2°C, NC shows a cold bias of 0.4°C and NE shows a cold bias of 1.4°C. The WH region has a much larger cold bias of 4.3°C. During JJA there are slightly higher warm biases across most regions of 1.0°C (IP), 2.1°C (NW), 0.5°C (WC), 0.6°C (EC), and 2.5°C (NC). The WH and NE have a cold bias of 2.8°C and 0.3°C, respectively. Both for annual and JJA periods there is an increase in Tmean between NF and FF for all SSPs over all regions. There is a small
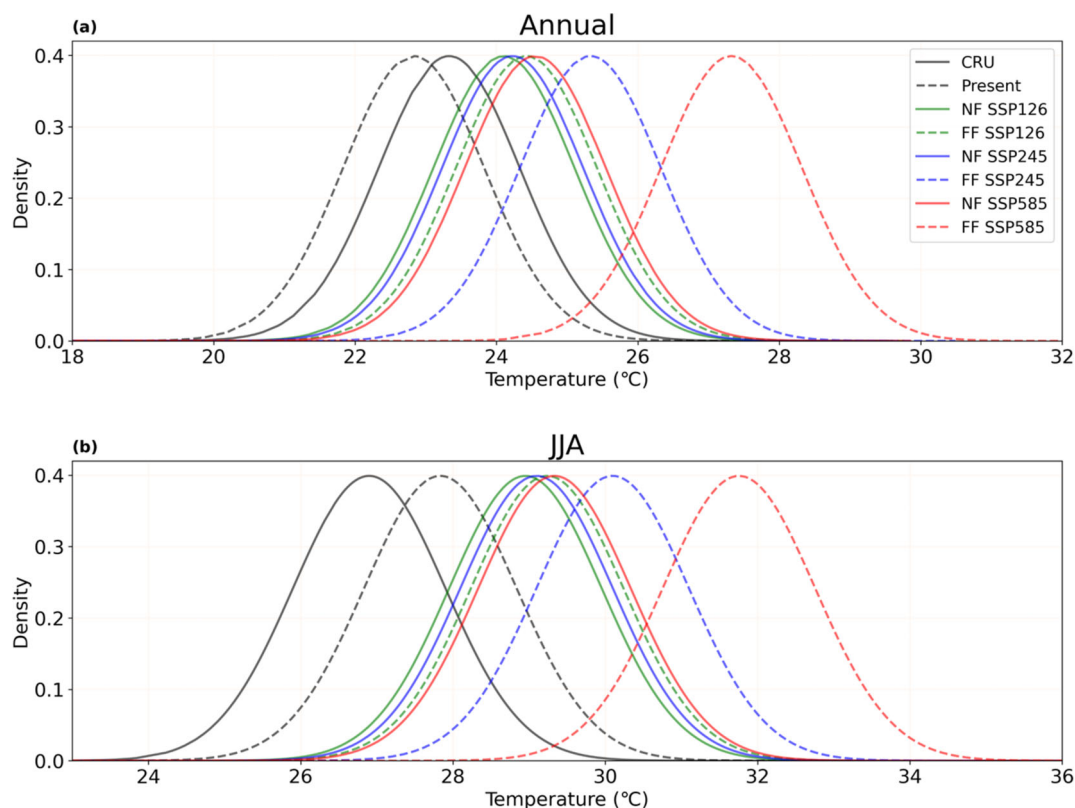
FIGURE 7 Annual (a) and JJA (b) mean near surface temperature over India. The solid grey line shows observed temperature, and the dashed grey line shows the present ensemble mean temperature for the historical period (1984–2014). The green, blue and red lines represent SSP1-2.6, SSP2-4.5, and SSP5-8.5. For the SSPs a solid line represents the NF (2030–2060), and a dashed line represents the FF (2070–2100). [Colour figure can be viewed at wileyonlinelibrary.com]

increase between NF and FF SSP1-2.6 and SSP2-4.5. The difference between NF and FF SSP5-8.5 is larger than the other two scenarios and FF SSP5-8.5 shows the highest shift in Tmean compared to observed values. The largest increases in Tmean are shown by FF SSP5-8.5, with an annual increase of 4.3°C (IP), 5.6°C (WH), 4.8°C (NW), 4.0°C (WC), 3.7°C (EC), 4.3°C (NE), and 4.6°C (NC) when compared to the historical Tmean of the MME. This means that the largest shift in Tmean can be seen over the WH region with the NW being close behind. JJA FF SSP5-8.5 compared to the historical Tmean of the MME shows an increase of 3.8°C (IP), 5.6°C (WH), 4.0°C (NW), 3.6°C (WC), 3.6°C (EC), 3.6°C (NE), and 3.8°C (NC). When looking at NF Tmean changes the WH, and NW regions show the largest shift from both annual and JJA Tmean of 2.3°C and 1.9°C (annual) and 2.5°C and 1.5°C (JJA) respectively under SSP5-8.5.

The MME of NF and FF changes in JJA Tmax for all the scenarios over India compared to the present is shown in Figure 9. The difference in temperature ranges from <1°C to >6°C over different regions under various scenarios. The regions that show strong differences are

the WH, east of NW, west of NC, west and central IP, and parts of EC and NE regions. All SSPs over all regions show warming compared to the present Tmax and there is warming when comparing NF SSP1-2.6, SSP2-4.5, SSP5-8.5, and FF SSP1-2.6, SSP2-4.5, SSP5-8.5, respectively, with the increase in temperature being the largest between NF and FF SSP5-8.5. Under FF SSP5-8.5 parts of the Western Himalaya region are projected to warm by over 6°C and all other regions show a warming of 4–6°C when compared to present-day temperatures. The warming is much lower for FF SSP1-2.6 and SSP2-4.5 with an increase over India of 1–3°C and 2–5°C, respectively. NF SSP5-8.5 shows similar warming to FF SSP1-2.6 meaning that SSP5-8.5 is projected to reach the same temperature increase as FF SSP1-2.6 30 years earlier.

In order to further investigate the rising temperatures, we analysed the JJA and annual time series averaged over India for all the variables, as shown in Figures 10 and S4 respectively. Comparing the observed series for the period 1984–2015, the MME series are consistently warmer than the observation for all the present years. This is due to the fact that MME are warmer over major parts of India as discussed previously. However, for the
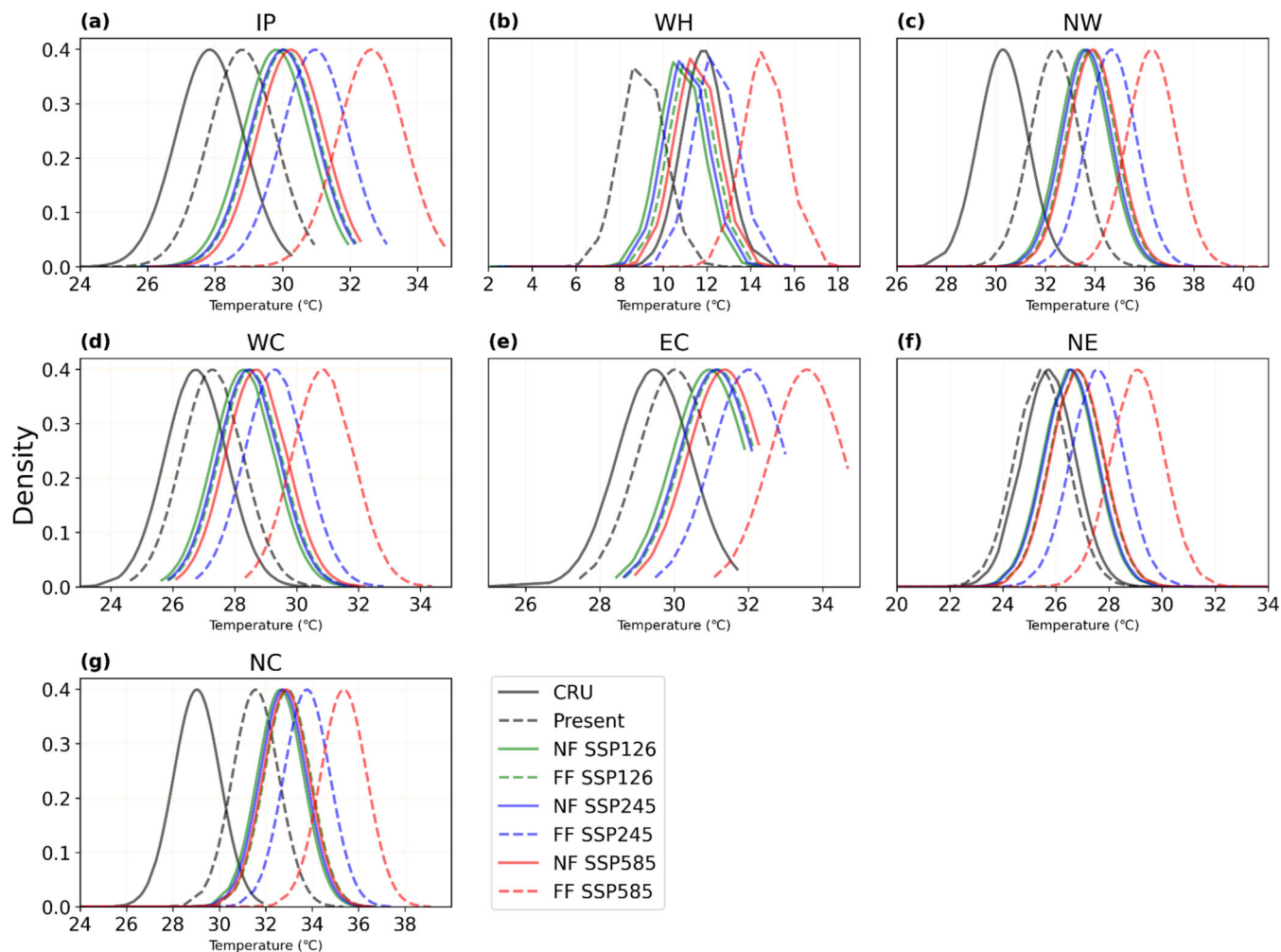
FIGURE 8   JJA mean near surface temperature for each temperature homogenous region over India. The solid grey line shows observed temperature, and the dashed grey line shows the present ensemble mean temperature for the historical period (1984–2014). The green, blue and red lines represent SSP1-2.6, SSP2-4.5, and SSP5-8.5. For the SSP scenarios a solid line represents the NF (2030–2060), and a dashed line represents the FF (2070–2100). [Colour figure can be viewed at wileyonlinelibrary.com]

annual timeseries (Figure S4) the MME annual means are colder than the observation. However, such differences are not much profound for the annual series. Annual Tmean is projected to increase by 1.3, 1.4, and 1.7°C for NF and 1.6, 2.5, and 4.5°C for FF. The annual Tmax is projected to increase by 1.1, 1.2, and 1.6°C for NF and 1.5, 2.3, and 4.1°C for FF. The annual Tmin is projected to increase by 1.4, 1.6, and 2.0°C for NF and 1.7, 2.7, and 5°C for FF. The above values are for SSP1-2.6, SSP2-4.5, and SSP5-8.5, respectively, and compare the mean of the NF and FF temperatures to the mean of the historical period. The SSPs show relatively similar temperatures till around 2040. The temperature rises for SSP1-2.6 levels off at around 2060 and the temperature rise for SSP2-4.5 decreases, almost levelling off by 2100, however, the temperature for SSP5-8.5 continues to steadily rise until the end of the century. A similar plot was created using the JJA period (Figure 10). During the

JJA period the MME over-predicts the temperature for Tmax, Tmean, and Tmin. JJA Tmean is projected to increase by 1.2, 1.3, and 1.5°C for NF and 1.4, 2.3, and 4°C for FF. The JJA Tmax is projected to increase by 0.9, 1.1, and 1.3°C for NF and 1.3, 2.1, and 3.7°C for FF. The JJA Tmin is projected to increase by 1.2, 1.4, and 1.7°C for NF and 1.4, 2.3, and 4.1°C for FF. The above values are for SSP1-2.6, SSP2-4.5, and SSP5-8.5 respectively. Annual and JJA periods show similar temperature increases for all SSPs. As expected, SSP5-8.5 shows the greatest increase in temperature by the end of the century for all temperatures for both annual and JJA periods. All SSPs show a higher temperature than present day showing that warming is inevitable, but the amount of warming can be reduced significantly with sufficient mitigation strategies. Similar increases in annual Tmean over India can be seen in Almazroui et al. (2021).
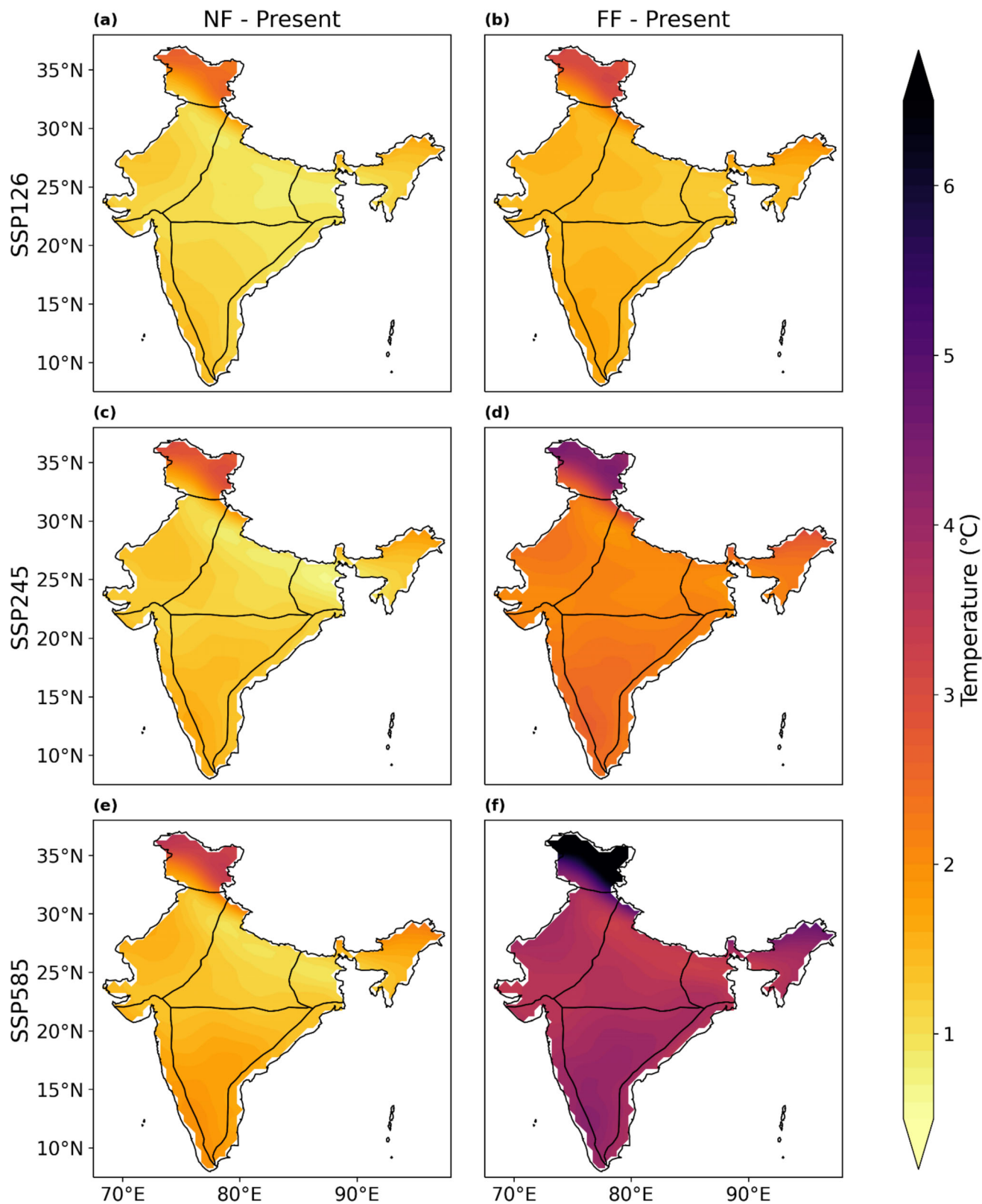
FIGURE 9 The difference in JJA Tmax for each SSP1-2.6 (a), (b), SSP2-4.5 (c), (d) and SSP5-8.5 (e), (f) compared to the historical period from the ensemble mean. The first columns (a), (c), (e) show the NF difference, and the second columns (b), (d), (f) show the FF difference. [Colour figure can be viewed at wileyonlinelibrary.com]
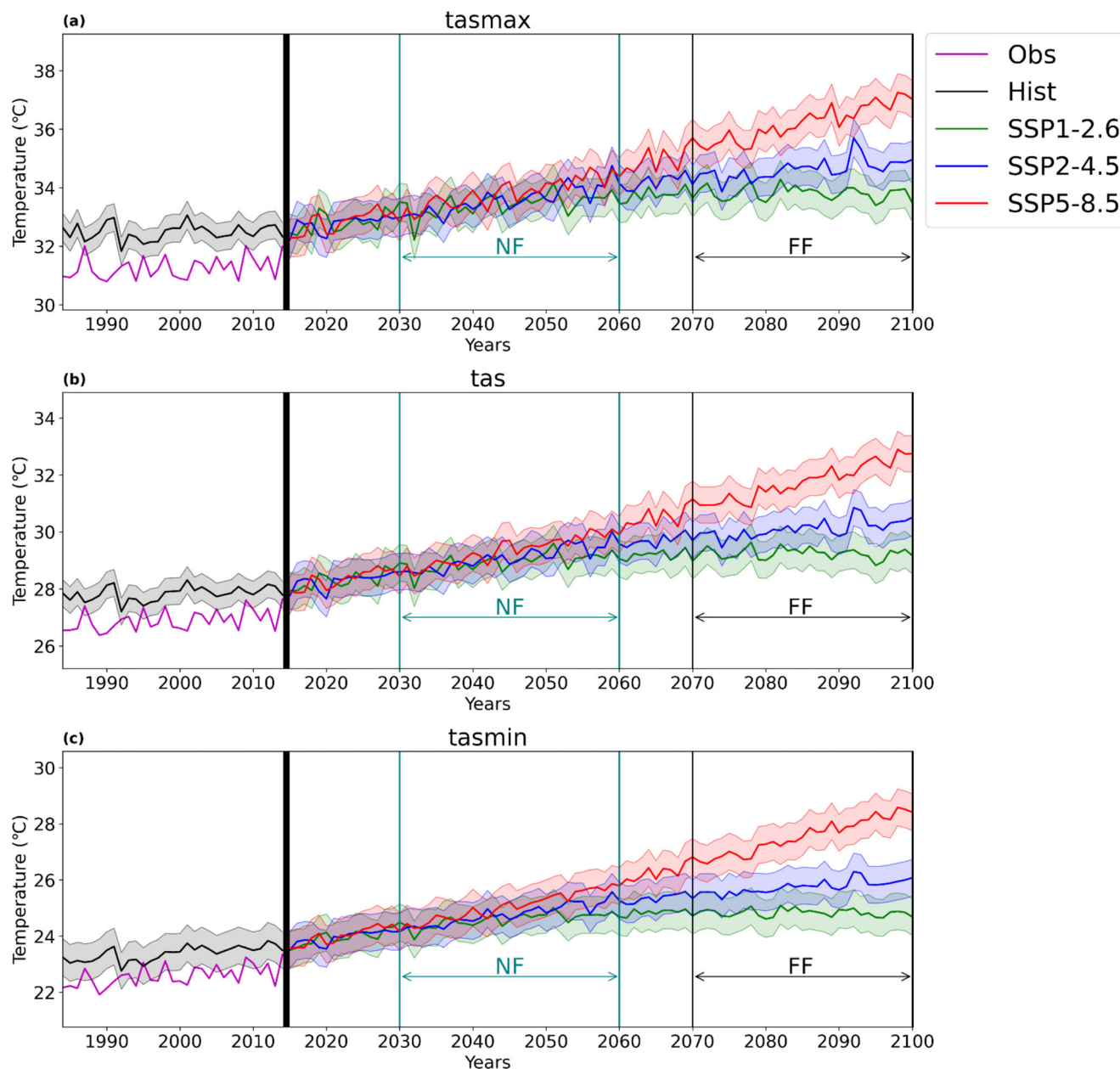
FIGURE 10 JJA maximum (a), mean (b) and minimum (c) near surface temperature over India for historical (1984–2014) and future (2015–2100). The magenta line is the observed temperature, and all others are an ensemble mean of 13 CMIP6 models. Near future (NF) is shown from 2030 to 2060 and far future (FF) is shown from 2070 to 2100. Grey represents the historical time period, and the green, blue and red lines represent SSP1-2.6, SSP2-4.5, and SSP5-8.5 respectively. [Colour figure can be viewed at wileyonlinelibrary.com]

The changes in the consecutive summer days are projected to decrease for the NF and increase for the FF over India for all SSPs when compared to the historical period (Figure 11). In the near future, the NC, east of NW, and west of NE regions show the largest decrease of around 30–40 consecutive summer days for all SSPs. Parts of the IP and EC also show a slightly lower decrease of around 10–20 days. The bottom of the IP and the west of the NW regions show a slight increase in consecutive summer days, with SSP5 showing the largest increase of 5–

20 days. The WH, west of the NE and WC regions appears to be unchanged for the NF. When looking at the FF period there is mostly an increase over India, with FF SSP5-8.5 showing the largest increase in consecutive summer days when compared to the historical period. The regions that see the largest increase are north of the NC, parts of NW, and northeast of NE across all SSPs, however FF SSP5-8.5 shows much higher areas of increased days in the EC and IP (60–80 days) compared to the other SSPs. A higher concentration of increased
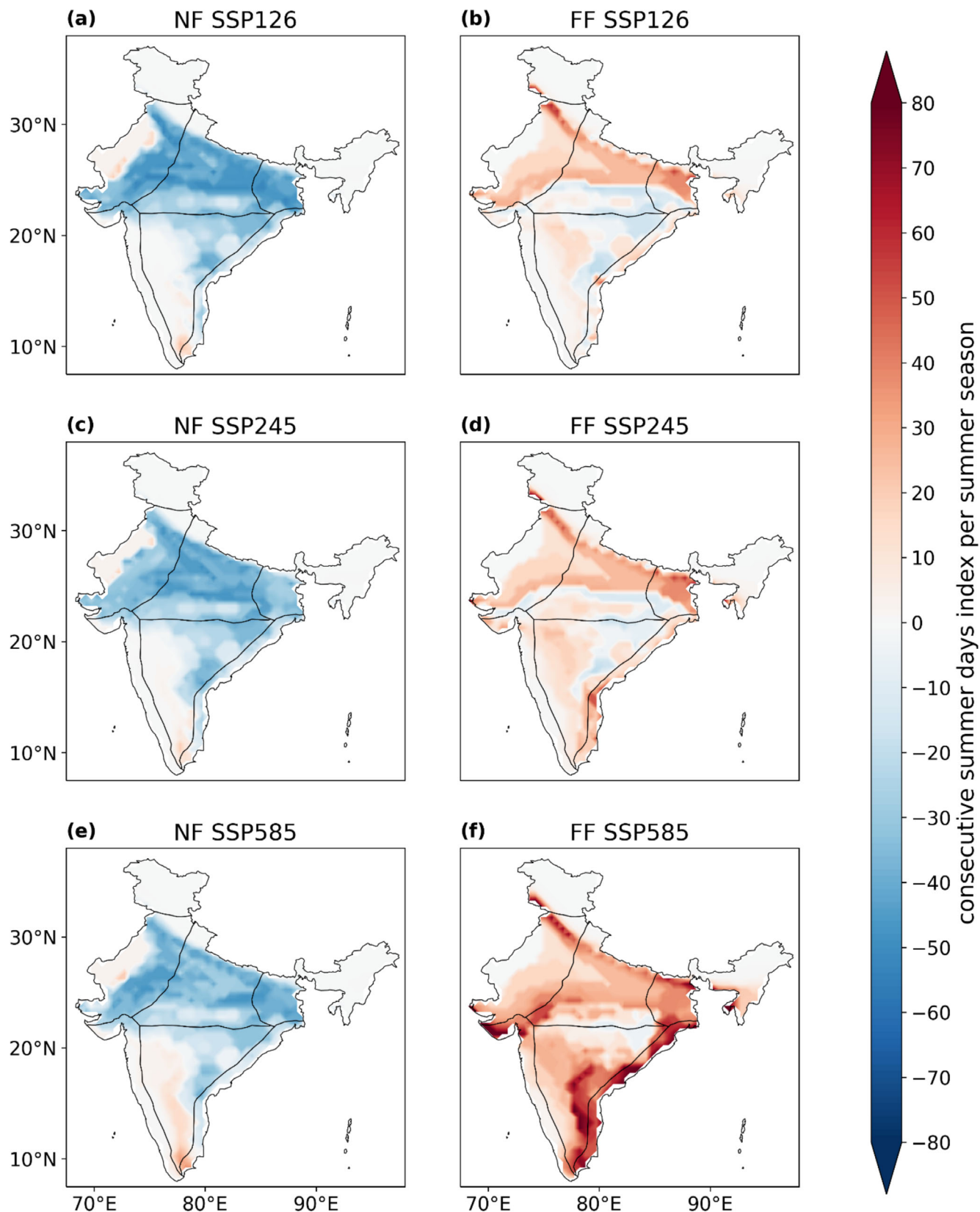
FIGURE 11 Consecutive summer days index per summer season difference compared to the ensemble mean of the historical period (1984–2014) for SSP1-2.6 (a), (b), SSP2-4.5 (c), (d), and SSP5-8.5 (e), (f). The first column shows the difference over the NF period (a), (c), (e) and the second column shows the difference over the FF period (b), (d), (f). [Colour figure can be viewed at wileyonlinelibrary.com]
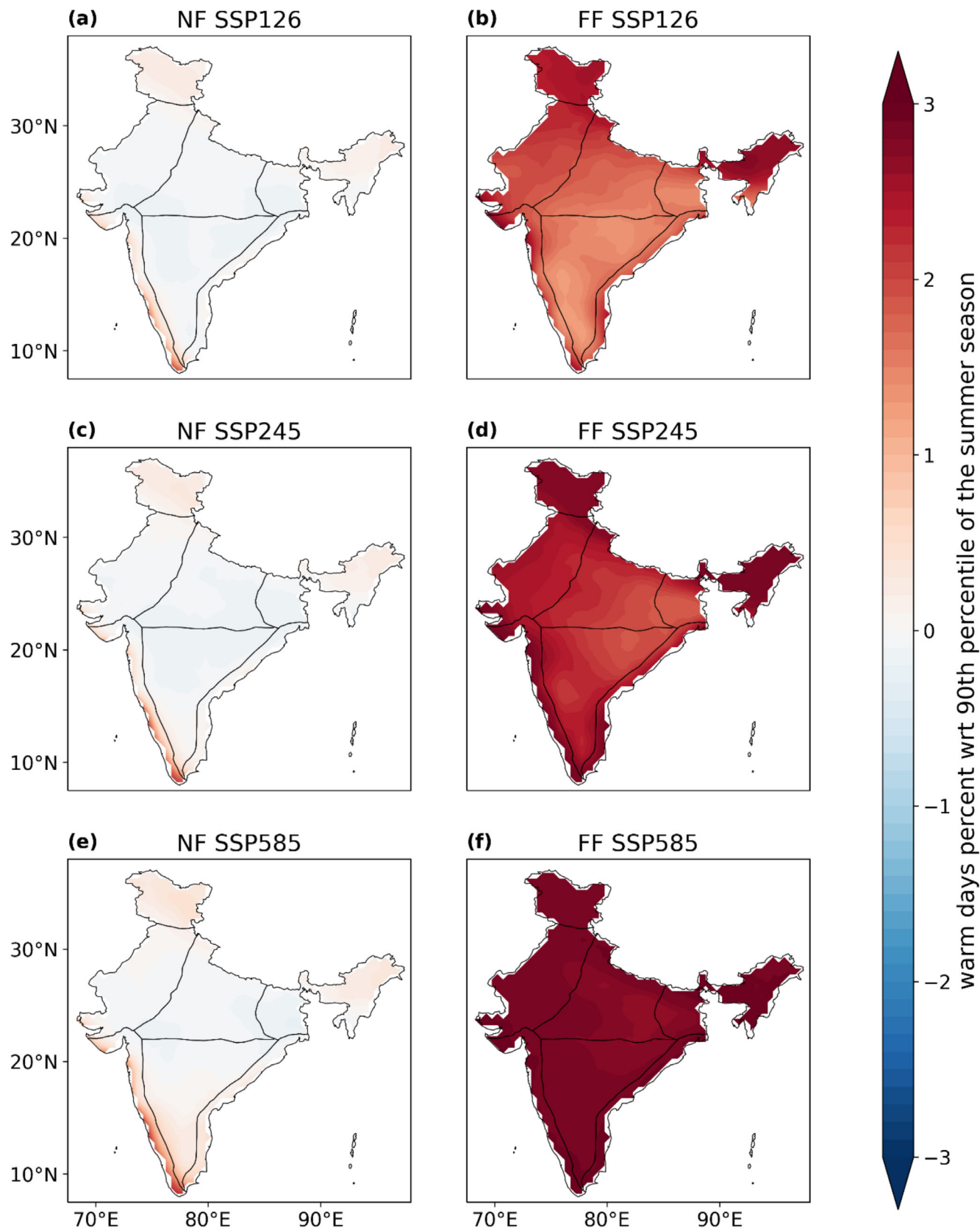
FIGURE 12   Warm days percent with reference to the 90th percentile of the summer season difference compared to the ensemble mean of the historical period (1984–2014) for SSP1-2.6 (a), (b), SSP2-4.5 (c), (d) and SSP5-8.5 (e), (f). The first column shows the difference over the NF period (a), (c), (e) and the second column shows the difference over the FF period (b), (d), (f). [Colour figure can be viewed at wileyonlinelibrary.com]
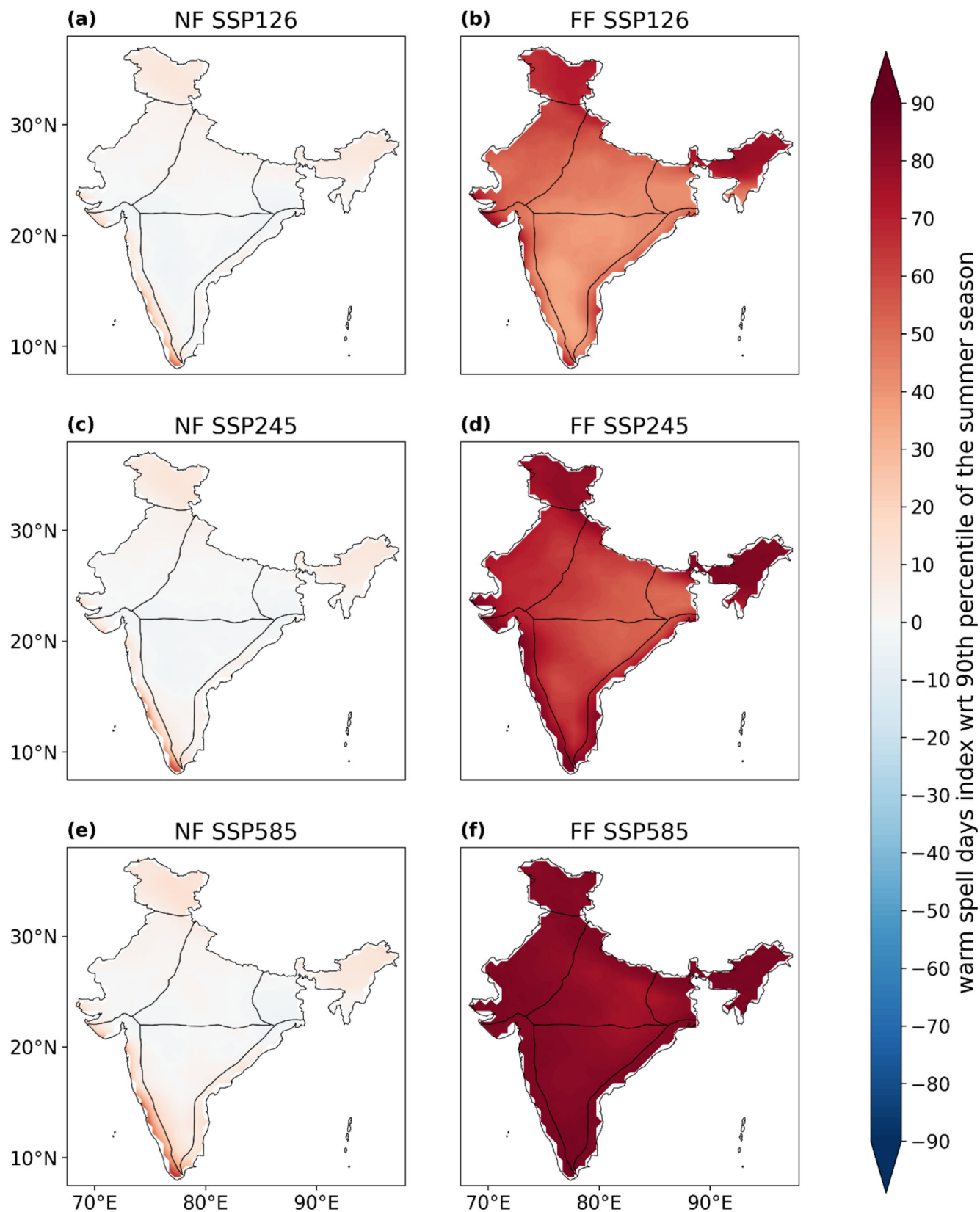
FIGURE 13 Warm spell days index with reference to the 90th percentile of the summer season difference compared to the ensemble mean of the historical period (1984–2014) for SSP1-2.6 (a), (b), SSP2-4.5 (c), (d) and SSP5-8.5 (e), (f). The first column shows the difference over the NF period (a), (c), (e) and the second column shows the difference over the FF period (b), (d), (f). [Colour figure can be viewed at wileyonlinelibrary.com]
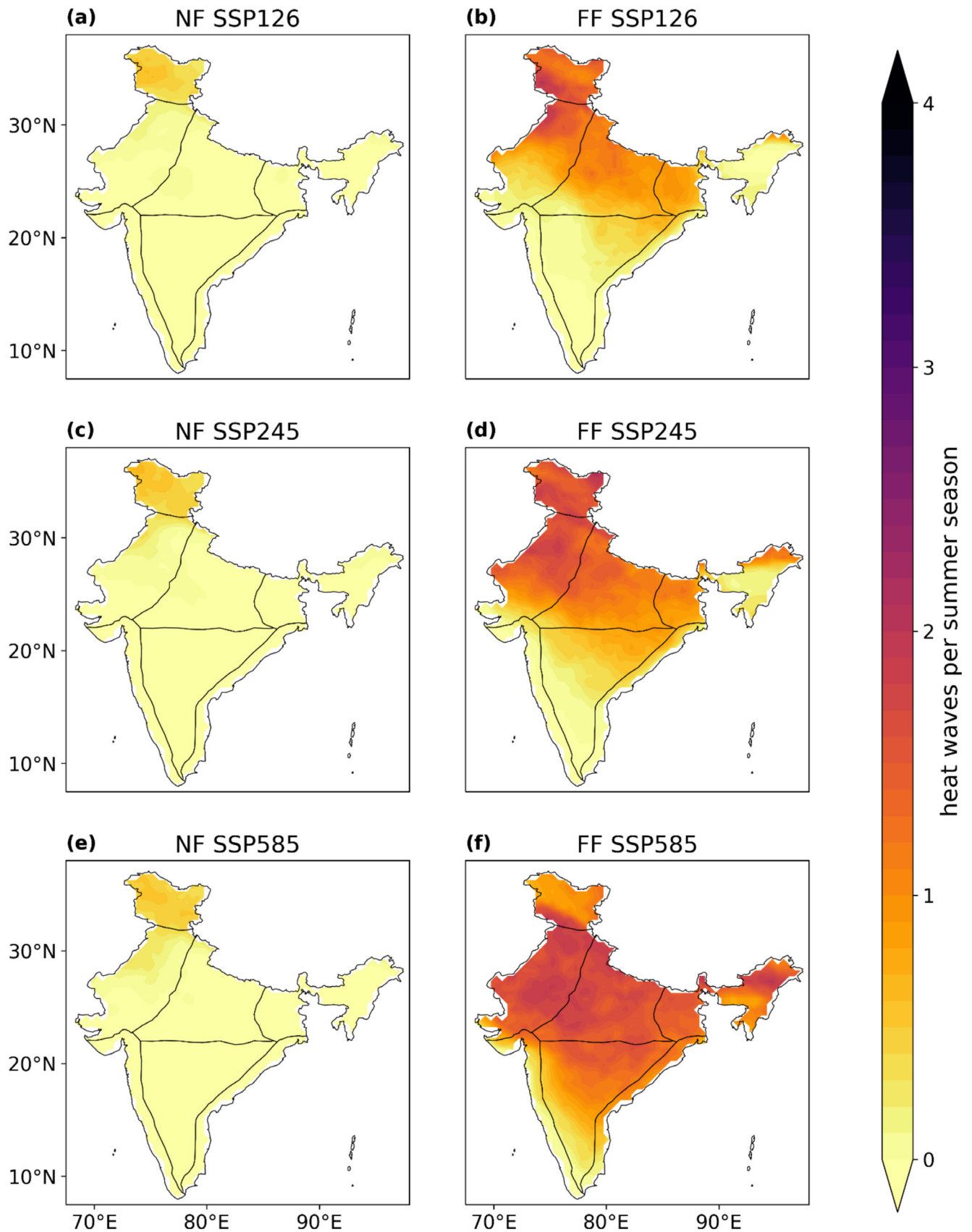
FIGURE 14 Legend on next page.

consecutive summer days seems to follow the Indo-Gangetic plains for FF. FF SSP1-2.6 and SSP2-4.5 show a slight decrease in parts of the NC and IP regions.

There is little change to the warm day's percent (Figure 12) during NF and an increase during the FF period for all SSPs when compared to the historical period. The WC shows the largest increase (1%) in warm days for all NF SSPs. There is a slight decrease in warm days for IP, NC, NW, and west of NE regions and a slight increase for WH, east of NE, and EC regions. All regions during FF SSPs show an increase in warm days percentage. The most affected regions for FF SSP1-2.6 and SSP2-4.5 are the WH, NE, and NW regions with SSP2-4.5 showing a larger percentage increase (2%–3%) when compared to SSP1-2.6. FF SSP5-8.5 shows the largest increase in warm days percent with most regions showing a 3 + % increase. East of the NC shows a slightly smaller increase (2.5%–3%) when compared to the other regions. The difference in warm spell days index (Figure 13) shows very similar spatial patterns as described above in Figure 12. Again, there is only a small change during the NF and a much larger increase during FF. The largest increase is seen in FF SSP5-8.5 which shows around 90 more warm spell days when compared to the historical period. FF SSP1-2.6 shows an increase of 30–60 days and FF SSP2-4.5 shows an increase of 50–70 days.

Both the heat wave frequency (Figures 14, S5, and S6) and duration (Figures 15, S7, and S8) are projected to increase by the end of the century over most parts of India. We have shown the number of heat waves per summer season for 3 (Figure S5), 5 (Figure S6), and 7 (Figure 14) consecutive days when compared to the historical period. When looking at 3 consecutive days, during the NF most regions (NC, NE, WC, IP, and EC) show no change in the number of heat waves for all SSPs. The WH region is most affected during the NF with around one more heat wave per summer season for all SSPs. There is a slight increase in parts of the NW where the coverage increases from SSP1-2.6 (least coverage) to SSP5-8.5 (most coverage). The same regions are affected for 5 and 7 days with the number of heat waves reducing slightly from 3 (1 day increase) to 7 (0.5-day increase) days. Moving onto the FF the increase in number of heat waves is much greater. The most affected regions for FF SSP1-2.6 are the WH, NW, and NC where parts of these regions project around 3 more heat waves per summer

season. Other parts of the NW, NC NE, IP, and EC show an increase of 2 heat waves per summer season. The least affected regions are the WC, southeast of the NE, and southwest of the IP. The number of heat waves increases when comparing SSP1-2.6 to the other two SSPs. FF SSP2-4.5 shows an increase in number of heat waves over most regions, with more parts of the NW, WH, NC, and northeast of the NE being the most affected (approx. 3 more heat waves per summer season). For FF SSP5-8.5 almost all regions show a coverage of 3+ more heat waves and the northeast of the NE shows the highest increase approaching 4 more heat waves. The WH region shows less of an increase (1–2 days) when compared to FF SSP1-2.6 and SSP2-4.5. The same patterns emerge with 5 and 7 consecutive day heat waves; however, the number of heat waves reduces with 3 consecutive day heat waves showing the highest increase (up to 4 more days), 5 consecutive heat wave days being in the middle (up to 2.5 more days) and 7 consecutive day heat waves showing the lowest increase (up to 2 more days) in heat wave days. Heat wave duration index (HWDI) is also shown for 3 (Figure S7), 5 (Figure S8), and 7 (Figure 15) consecutive day heat waves, although there is negligible differences between these figures. All regions except the WH show no increase in HWDI for all NF SSPs and the WH shows an increase of up to 15 more days. Larger increases are seen for all SSPs in the FF with SSP5-8.5 showing the largest increases. The WH region is the most affected with 55, 65, and 70 more days for SSPs 1, 2, and 5 respectively. The next most affected regions are the NW, NC, and NE which affect the most populated areas of India. These regions see an increase of 20, 30, and 50 more days for SSPs 1, 2, and 5 respectively. Whilst the EC, WC, and parts of the IP and NE are mostly unaffected for SSPs 1 and 2, SSP5-8.5 shows that all of India except the WC will have an increase in HWDI.

Overall, the analysis suggests that spatial temperature trends over India, CNRM-CM6 is the best performing GCM, although a lot of the GCMs (CMCC-ESM2, FIO-ESM-2-0, GFDL-ESM4) perform almost as well. When looking at the temporal temperature patterns over India HadGEM3-GC31-LL, KACE-1-0G, and UKESM1-0-LL perform much better than other GCMs. Our work has shown that the largest increase in future heat wave duration, intensity, and frequency is from FF SSP5-8.5. This is comparable to other studies over South Asia that have shown similar results using CMIP5 (Yang et al., 2020)

FIGURE 14 Heat waves per summer season (where TX > TXnorm +5°C for 7 consecutive days) difference compared to the ensemble mean of the historical period (1984–2014) for SSP1-2.6 (a), (b), SSP2-4.5 (c), (d) and SSP5-8.5 (e), (f). The first column shows the difference over the NF period (a), (c), (e) and the second column shows the difference over the FF period (b), (d), (f). [Colour figure can be viewed at wileyonlinelibrary.com]
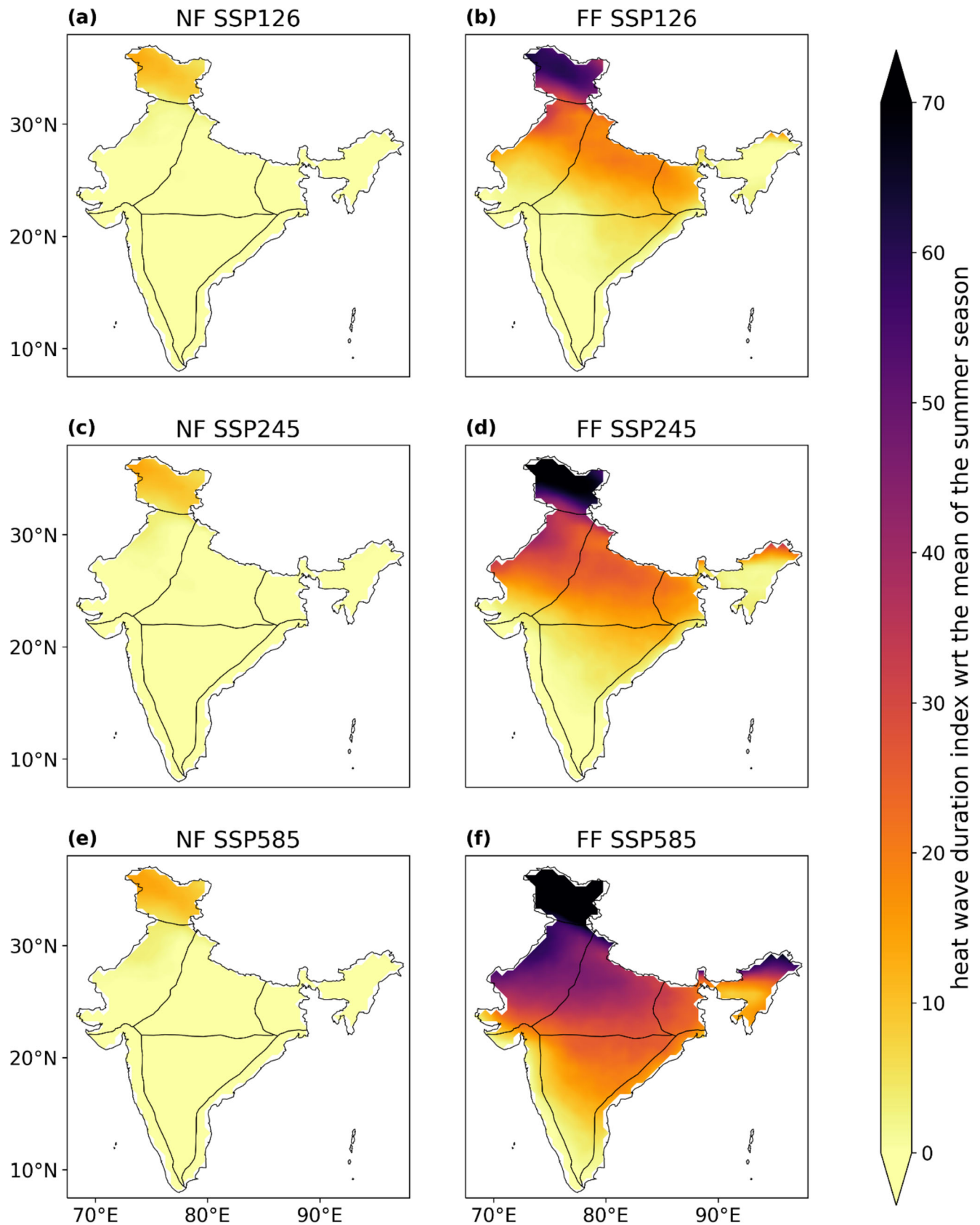
FIGURE 15 Heat wave duration index with reference to the mean of the summer season (where TX > TXnorm +5°C for 7 consecutive days) difference compared to the ensemble mean of the historical period (1984–2014) for SSP1-2.6 (a), (b), SSP2-4.5 (c), (d) and SSP5-8.5 (e), (f). The first column shows the difference over the NF period (a), (c), (e) and the second column shows the difference over the FF period (b), (d), (f). [Colour figure can be viewed at wileyonlinelibrary.com]

and CMIP6 models (Hamed et al., 2022; Salehie et al., 2022; Ullah et al., 2022, 2023).

4 | CONCLUSION

The fidelity of 13 CMIP6 models have been assessed for simulating the temperature over the Indian temperature homogenous regions. A new addition for CMIP6 models compared to previous version is the addition of SSP scenarios which were used to simulate the mean, maximum, and minimum temperature up to the end of the century. Our results indicate that:

- CMIP6 models do well at modelling the spatial distribution of temperature over Indian homogenous temperature regions, although they struggle with the colder temperatures of the Western Himalaya and Northeast regions due to the topographic complexity, snow cover, and reduced observed values which the coarse resolution of the models fails to capture.
- CNRM-CM6 performs best comparably to other models for spatial temperature over India. HadGEM3-GC31-LL, KACE-1-0G, and UKESM1-0-LL are comparably the best-performing models for temporal temperature trends over India.
- The MME tends to have a larger warm bias during the JJA period compared to the annual period for mean, maximum, and minimum temperature. This could suggest that the models are overestimating warm temperatures during JJA. There is more variation in the warm and cold biases of the MME per region for the annual period. The IP region has mostly a cold bias for annual temperatures. NC shows a warm bias for Tmax and Tmean but more of a cold bias for Tmin. NW shows a warm bias for Tmax and mostly a cold bias for Tmean and Tmin. The WH and NE show a large cold bias for all temperatures during annual and JJA periods.
- MME outperforms the individual models in terms of the mean biases for different temperature metrics.
- Both annual and JJA temperatures are shown to increase in the NF and FF for mean, maximum, and minimum temperatures. The annual maximum temperature is projected to increase by 1.1, 1.2, and 1.6°C for NF and 1.5, 2.3, and 4.1°C for FF SSP1-2.6, SSP2-4.5 and SSP5-8.5, respectively.
- All SSP scenarios project a higher mean, maximum, and minimum temperature by the end of the century suggesting that even with mitigation in place, warming is inevitable.
- The mean, maximum, and minimum temperature increase for both SSP1-2.6 and SSP2-4.5 seem to level off by the end of the century, whereas SSP5-8.5 continues to rise steadily. This suggests that with sufficient mitigation strategies, we can significantly limit the amount of warming over this region by the end of the century.
- Both the frequency and duration of heat waves are shown to increase in the FF with the most populated areas of India being the most affected. The increase shown by SSP1-2.6 is significantly less than what is seen by SSP5-8.5, meaning that effective mitigation can reduce both the frequency and duration of heat waves seen over India by the end of the century.

CONFLICT OF INTEREST STATEMENT
The authors declare no conflict of interests.

DATA AVAILABILITY STATEMENT
The data set can be downloaded using the link https://crudata.uea.ac.uk/cru/data/hrg/cru_ts_4.05 and https://esgf-node.llnl.gov/search/cmip6 respectively.

ORCID
P. R. Tiwari https://orcid.org/0000-0002-7580-0446
D. Kumar https://orcid.org/0000-0003-2253-4129

REFERENCES
Acharya, N., Chattopadhyay, S., Mohanty, U.C. & Ghosh, K. (2014) Prediction of Indian summer monsoon rainfall: a weighted multi-model ensemble to enhance probabilistic forecast skills. *Meteorological Applications*, 21(3), 724–732. Available from: https://doi.org/10.1002/met.1400

Almazroui, M., Ashfaq, M., Islam, M., Rashid, I., Kamil, S., Abid, M. et al. (2021) Assessment of CMIP6 performance and projected temperature and precipitation changes over South America. *Earth Systems and Environment*, 5(2), 155–183. Available from: https://doi.org/10.1007/s41748-021-00233-6

Arbuthnott, K.G. & Hajat, S. (2017) The health effects of hotter summers and heat waves in the population of the United Kingdom: A review of the evidence. *Environmental Health*, 16(S1), 119. Available from: https://doi.org/10.1186/s12940-017-0322-5

Ashfaq, M., Cavazos, T., Reboita, M.S., Torres-Alavez, J.A., Im, E.S., Olusegun, C.F. et al. (2021) Robust late twenty-first century shift in the regional monsoons in RegCM-CORDEX simulations. *Climate Dynamics*, 57, 1463–1488. Available from: https://doi.org/10.1007/s00382-020-05306-2

Bandara, J.S. & Cai, Y. (2014) The impact of climate change on food crop productivity, food prices and food security in South Asia. *Economic Analysis and Policy*, 44(4), 451–465. Available from: https://doi.org/10.1016/j.eap.2014.09.005

Collins, M., Knutti, R., Arblaster, J., Dufresne, J.-L., Fichefet, T., Friedlingstein, P. et al. (2013) Long-term climate change: projections, commitments and irreversibility. In: Stocker, T.F., Qin, D., Plattner, G.-K., Tignor, M., Allen, S.K., Boschung, J. et al. (Eds.) *Climate change 2013: the physical science basis. Contribution of working group I to the fifth assessment report of the intergovernmental panel on climate change.* Cambridge, UK and New York, NY, USA: Cambridge University Press.

Das, S., Giorgi, F., Coppola, E., Panicker, A.S., Gautam, A.S., Nair, V.S. et al. (2021) Linkage between the absorbing aerosol-induced snow darkening effects over the Himalayas-Tibetan plateau and the pre-monsoon climate over northern India. *Theoretical and Applied Climatology*, 147(3–4), 1033–1048. Available from: https://doi.org/10.1007/s00704-021-03871-y

Dey, S. & Di Girolamo, L. (2010) A decade of change in aerosol properties over the Indian subcontinent. *Geophysical Research Letters*, 38, L14811. Available from: https://doi.org/10.1029/2011GL048153

Dash, S.K. & Mamgain, A. (2011) Changes in the frequency of different categories of temperature extremes in India. *Journal of Applied Meteorology and Climatology*, 50(9), 1842–1858. Available from: https://doi.org/10.1175/2011jamc2687.1

De, U.S., Dube, R.K. & Prakasa Rao, G.S. (2005) Extreme weather events over India in the last 100 years. *Journal of the Indian Geophysical Union*, 9, 173–187.

Dileepkumar, R., AchutaRao, K. & Arulalan, T. (2018) Human influence on sub-regional surface air temperature change over India. *Scientific Reports*, 8(1), 8967. Available from: https://doi.org/10.1038/s41598-018-27185-8

Dippoliti, D., Michelozzi, P., Marino, C., de Donato, F., Menne, B., Katsouyanni, K. et al. (2010) The impact of heat waves on mortality in 9 European cities: results from the EuroHEAT project. *Environmental Health*, 9, 37. Available from: https://doi.org/10.1186/1476-069x-9-37

Dong, Z., Wang, L., Sun, Y., Hu, T., Limsakul, A., Singhruck, P. et al. (2021) Heatwaves in Southeast Asia and their changes in a warmer world. Earth's. *Futures*, 9(7), e2021EF001992. Available from: https://doi.org/10.1029/2021ef001992

Eyring, V., Bony, S., Meehl, G.A., Senior, C.A., Stevens, B., Stouffer, R.J. et al. (2016) Overview of the coupled model intercomparison project phase 6 (CMIP6) experimental design and organization. *Geoscientific Model Development*, 9(5), 1937–1958. Available from: https://doi.org/10.5194/gmd-9-1937-2016

Gornall, J., Betts, R., Burke, E., Clark, R., Camp, J., Willett, K. et al. (2010) Implications of climate change for agricultural productivity in the early twenty-first century. *Philosophical Transactions of the Royal Society B: Biological Sciences*, 365(1554), 2973–2989. Available from: https://doi.org/10.1098/rstb.2010.0158

Haines, A., Kovats, R.S., Campbell-Lendrum, D. & Corvalan, C. (2006) Climate change and human health: impacts, vulnerability and public health. *Public Health*, 120(7), 585–596. Available from: https://doi.org/10.1016/j.puhe.2006.01.002

Hamed, M.M., Nashwan, M.S., Shahid, S., bin Ismail, T., Dewan, A. & Asaduzzaman, M. (2022) Thermal bioclimatic indicators over Southeast Asia: present status and future projection using CMIP6. *Environmental Science and Pollution Research*, 29, 91212–91231. Available from: https://doi.org/10.1007/s11356-022-22036-6

Harris, I., Jones, P.D., Osborn, T.J. & Lister, D.H. (2013) Updated high-resolution grids of monthly climatic observations—the CRU TS3.10 dataset. *International Journal of Climatology*, 34(3), 623–642. Available from: https://doi.org/10.1002/joc.3711

IPCC. (2022) In: Shukla, P.R., Skea, J., Slade, R., al Khourdajie, A., van Diemen, R., McCollum, D. et al. (Eds.) *Climate change 2022: mitigation of climate change. Contribution of working group III to the sixth assessment report of the intergovernmental panel on climate change.* Cambridge, UK and New York, NY, USA: Cambridge University Press. Available from: https://doi.org/10.1017/9781009157926

Kanda, N., Negi, H.S., Rishi, M.S. & Kumar, A. (2020) Performance of various gridded temperature and precipitation datasets over northwest Himalayan region. *Environmental Research Communications*, 2(8), 085002. Available from: https://doi.org/10.1088/2515-7620/ab9991

Kumar, P., Wiltshire, A., Mathison, C., Asharaf, S., Ahrens, B., Lucas-Picher, P. et al. (2013) Downscaled climate change projections with uncertainty assessment over India using a high-resolution multi-model approach. *Science of the Total Environment*, 468–469, S18–S30. Available from: https://doi.org/10.1016/j.scitotenv.2013.01.051

Maharana, P., Younous, A. & Pattnayak, K. (2018) Observed climate variability over Chad using multiple observational and reanalysis datasets. *Global and Planetary Change*, 162, 252–265. Available from: https://doi.org/10.1016/j.gloplacha.2018.01.013

Mazdiyasni, O., AghaKouchak, A., Davis, S.J., Madadgar, S., Mehran, A., Ragno, E. et al. (2017) Increasing probability of mortality during Indian heat waves. *Science Advances*, 3(6), 1700066. Available from: https://doi.org/10.1126/sciadv.1700066

Meehl, G.A. & Tebaldi, C. (2004) More intense, more frequent, and longer lasting heat waves in the 21st century. *Science*, 305(5686), 994–997. Available from: https://doi.org/10.1126/science.1098704

Mitchell, T.D. & Jones, P.D. (2005) An improved method of constructing a database of monthly climate observations and associated high-resolution grids. *International Journal of Climatology*, 25(6), 693–712. Available from: https://doi.org/10.1002/joc.1181

Moss, R.H., Edmonds, J.A., Hibbard, K.A., Manning, M.R., Rose, S.K., van Vuuren, D.P. et al. (2010) The next generation

of scenarios for climate change research and assessment. *Nature*, 463(7282), 747–756. Available from: https://doi.org/10.1038/nature08823

O'Neill, B.C., Kriegler, E., Ebi, K.L., Kemp-Benedict, E., Riahi, K., Rothman, D.S. et al. (2017) The roads ahead: narratives for shared socioeconomic pathways describing world futures in the 21st century. *Global Environmental Change*, 42, 169–180. Available from: https://doi.org/10.1016/j.gloenvcha.2015.01.004

Pai, D., Nair, S. & Ramanathan, A. (2013) Long term climatology and trends of heat waves over India during the recent 50 years (1961-2010). *Mausam*, 64(4), 585–604. Available from: https://doi.org/10.54302/mausam.v64i4.742

Panda, S.K., Hong, M., Dash, S.K., Jai-Ho, O. & Pattnayak, K.C. (2020) Relative roles of Eurasian snow depth and sea surface temperature in Indian and Korean summer monsoons based on GME model simulations. *Earth and Space Science*, 7, e2020EA001105. Available from: https://doi.org/10.1029/2020EA001105

Pattnayak, K.C., Abdel, A.Y., Rathakrishnan, K.V., Singh, M., Dash, R. & Maharana, P. (2019) Changing climate over Chad: is the rainfall over the major cities recovering? *Earth and Space Science*, 6(7), 1149–1160.

Pattnayak, K.C., Kar, S.C., Dalal, M. & Pattnayak, R. (2017) Projections of annual rainfall and surface temperature from CMIP5 models over the BIMSTEC countries. *Global and Planetary Change*, 152, 152–166. Available from: https://doi.org/10.1016/j.gloplacha.2017.03.005

Patz, J.A., Campbell-Lendrum, D., Holloway, T. & Foley, J.A. (2005) Impact of regional climate change on human health. *Nature*, 438(7066), 310–317. Available from: https://doi.org/10.1038/nature04188

Perkins, S.E. & Alexander, L.V. (2013) On the measurement of heat waves. *Journal of Climate*, 26(13), 4500–4517. Available from: https://doi.org/10.1175/jcli-d-12-00383.1

Ray, K., Giri, R.K., Ray, S.S., Dimri, A.P. & Rajeevan, M. (2021) An assessment of long-term changes in mortalities due to extreme weather events in India: A study of 50 years' data, 1970–2019. *Weather and Climate Extremes*, 32, 100315. Available from: https://doi.org/10.1016/j.wace.2021.100315

Riahi, K., van Vuuren, D.P., Kriegler, E., Edmonds, J., O'Neill, B.C., Fujimori, S. et al. (2017) The shared socioeconomic pathways and their energy, land use, and greenhouse gas emissions implications: an overview. *Global Environmental Change*, 42, 153–168. Available from: https://doi.org/10.1016/j.gloenvcha.2016.05.009

Rohini, P., Rajeevan, M. & Srivastava, A.K. (2016) On the variability and increasing trends of heat waves over India. *Scientific Reports*, 6(1), 26153. Available from: https://doi.org/10.1038/srep26153

Salehie, O., bin Ismail, T., Hamed, M.M., Shahid, S. & Idlan Muhammad, M.K. (2022) Projection of hot and cold extremes in the Amu River basin of Central Asia using GCMs CMIP6. *Stochastic Environmental Research and Risk Assessment*, 36, 3395–3416. Available from: https://doi.org/10.1007/s00477-022-02201-6

Schulzweida, U. (2021) CDO User Guide. (Version 2.0.0). Zenodo https://doi.org/10.5281/zenodo.5614769

Shahi, N.K., Das, S., Ghosh, S., Maharana, P. & Rai, S. (2021) Projected changes in the mean and intra-seasonal variability of the Indian summer monsoon in the RegCM CORDEX-CORE simulations under higher warming conditions. *Climate Dynamics*, 57, 1489–1506. Available from: https://doi.org/10.1007/s00382-021-05771-3

Sivakumar, M.V.K. & Stefanski, R. (2010) Climate change in South Asia. In: Lal, R., Sivakumar, M., Faiz, S., Mustafizur Rahman, A., & Islam, K. (Eds.) Climate change and food security in South Asia. Dordrecht: Springer, pp. 13–30. Available from: https://doi.org/10.1007/978-90-481-9516-9_2

Stouffer, R.J., Eyring, V., Meehl, G.A., Bony, S., Senior, C., Stevens, B. et al. (2017) CMIP5 scientific gaps and recommendations for CMIP6. *Bulletin of the American Meteorological Society*, 98(1), 95–105. Available from: https://doi.org/10.1175/bams-d-15-00013.1

Taylor, K., Stouffer, R. & Meehl, G. (2012) An overview of CMIP5 and the experiment design. *Bulletin of the American Meteorological Society*, 93(4), 485–498. Available from: https://doi.org/10.1175/BAMS-D-11-00094.1

Taylor, K.E. (2001) Summarizing multiple aspects of model performance in a single diagram. *Journal of Geophysical Research: Atmospheres*, 106, 7183–7192. Available from: https://doi.org/10.1029/2000jd900719

Tiwari, P.R., Kar, S.C., Mohanty, U.C., Dey, S., Sinha, P., Raju, P.V.S. et al. (2016) On the dynamical downscaling and bias correction of seasonal-scale winter precipitation predictions over North India. *Quarterly Journal of the Royal Meteorological Society*, 142(699), 2398–2410. Available from: https://doi.org/10.1002/qj.2832

Tiwari, P.R., Kar, S.C., Mohanty, U.C., Dey, S., Sinha, P.C. & Shekhar, M.S. (2017) Sensitivity of the Himalayan orography representation in simulation of winter precipitation using regional climate model (RegCM) nested in a GCM. *Climate Dynamics*, 49(11–12), 4157–4170. Available from: https://doi.org/10.1007/s00382-017-3567-3

Ullah, S., You, Q., Chen, D., Sachindra, D.A., AghaKouchak, A., Kang, S. et al. (2022) Future population exposure to daytime and night-time heat waves in South Asia. *Earth's Future*, 10, e2021EF002511. Available from: https://doi.org/10.1029/2021ef002511

Ullah, S., You, Q., Ullah, W., Sachindra, D.A., Ali, A., Bhatti, A.S. et al. (2023) Climate change will exacerbate population exposure to future heat waves in the China-Pakistan economic corridor. *Weather and Climate Extremes*, 40, 100570. Available from: https://doi.org/10.1016/j.wace.2023.100570

Yang, Y., Jin, C. & Ali, S. (2020) Projection of heat wave in China under global warming targets of 1.5°C and 2°C by the ISIMIP models. *Atmospheric Research*, 244, 105057. Available from: https://doi.org/10.1016/j.atmosres.2020.105057

You, Q., Jiang, Z., Kong, L., Wu, Z., Bao, Y., Kang, S. et al. (2016) A comparison of heat wave climatologies and trends in China based on multiple definitions. *Climate Dynamics*, 48(11–12), 3975–3989. Available from: https://doi.org/10.1007/s00382-016-3315-0

Zeng, Q., Li, G., Cui, Y., Jiang, G. & Pan, X. (2016) Estimating temperature-mortality exposure-response relationships and optimum ambient temperature at the Multi-City level of China. *International Journal of Environmental Research and Public Health*, 13(3), 279. Available from: https://doi.org/10.3390/ijerph13030279

Zhao, A., Bollasina, M.A. & Stevenson, D.S. (2019) Strong influence of aerosol reductions on future heatwaves. *Geophysical Research Letters*, 46(9), 4913–4923. Available from: https://doi.org/10.1029/2019gl082269

SUPPORTING INFORMATION

Additional supporting information can be found online in the Supporting Information section at the end of this article.